

Review

# Recent Advances in the Grain Refinement Effects of Zr on Mg Alloys: A Review

Ming Sun <sup>1</sup>, Depeng Yang <sup>1</sup>, Yu Zhang <sup>2,\*</sup>, Lin Mao <sup>3</sup>, Xikuo Li <sup>1</sup>  and Song Pang <sup>4</sup>

<sup>1</sup> School of Materials and Chemistry, University of Shanghai for Science and Technology, Shanghai 200093, China

<sup>2</sup> College of Materials Science and Engineering, Chongqing University, Chongqing 400044, China

<sup>3</sup> Shanghai Institute for Minimally Invasive Therapy, School of Health Science and Engineering, University of Shanghai for Science and Technology, Shanghai 200093, China

<sup>4</sup> Shanghai Metal Materials Near-Net-Shape Engineering Research Center, Shanghai Spaceflight Precision Machinery Institute, Shanghai 201600, China

\* Correspondence: yu.zhang@cqu.edu.cn

**Abstract:** As the lightest structural materials, Mg alloys show great effectiveness at energy saving and emission reduction when applied in the automotive and aerospace fields. In particular, Zr-bearing Mg alloys (non-Al containing) exhibit high strengths and elevated-temperature usage values. Zr is the most powerful grain refiner, and it provides fine grain sizes, uniformities in microstructural and mechanical properties and processing formability for Mg alloys. Due to the importance of Zr alloying, this review paper systematically summarizes the latest research progress in the grain refinement effects of Zr on Mg alloys. The main points are reviewed, including the alloying process of Zr, the grain refinement mechanism of Zr, factors affecting the grain refinement effects of Zr, and methods improving grain refinement efficiency of Zr. This paper provides a comprehensive understating of grain refinement effects of Zr on Mg alloys for the researchers and engineers.

**Keywords:** magnesium alloy; Mg-Zr master alloy; Zr refiner; grain refinement; casting



**Citation:** Sun, M.; Yang, D.; Zhang, Y.; Mao, L.; Li, X.; Pang, S. Recent Advances in the Grain Refinement Effects of Zr on Mg Alloys: A Review. *Metals* **2022**, *12*, 1388. <https://doi.org/10.3390/met12081388>

Academic Editor: Dmytro Orlov

Received: 5 July 2022

Accepted: 19 August 2022

Published: 21 August 2022

**Publisher's Note:** MDPI stays neutral with regard to jurisdictional claims in published maps and institutional affiliations.



**Copyright:** © 2022 by the authors. Licensee MDPI, Basel, Switzerland. This article is an open access article distributed under the terms and conditions of the Creative Commons Attribution (CC BY) license (<https://creativecommons.org/licenses/by/4.0/>).

## 1. Introduction

Due to low densities and high specific strengths, Mg alloys show great potential in aerospace and automobile areas because the application of Mg alloys to structural components can effectively reduce weight, fuel consumption and CO<sub>2</sub> emissions [1,2]. However, the mechanical properties of Mg alloys are relatively low, and require further improvement by means of various strengthening methods. During the casting process of Mg alloys, grain refinement is one of the most important steps for improving castability, microstructure uniformity, mechanical properties, and post-formability [3,4]. In particular, the low ductility of Mg alloys due to the hexagonal close-packed (HCP) crystal structure can be effectively improved by grain refinement.

On the basis of differences in the grain refinement method employed, Mg alloys can be roughly divided into two groups, i.e., Al-bearing and Al-free Mg alloys. For the Al-bearing Mg alloys, there are still no ideal grain refiners [4]. Conversely, for Al-free Mg alloys, Zr has become the most effective grain refiner since it was found in the 1940s by Sauerwald [5]. Driven by the needs of aircraft components, Zr-containing Mg alloys with higher strengths and elevated temperature resistances have been developed [6,7] that take advantage of grain refinement, the precipitation strengthening effect, and other strengthening factors [8]. For example, WE43 alloy (Mg-4% Y-3% RE-0.5% Zr, RE = rare earth) shows high strength and long-term thermal stability at temperatures as high as 250 °C [6], and Mg-8Gd-4Y-0.8Zr alloy exhibits a better creep resistance than WE54 at an applied stress of 100 MPa and temperatures from 250 °C to 300 °C [7], which can be applied

in military and aerospace areas [9]. Thus, it is believed that without the grain refiner Zr, the development of high-strength Mg alloys remains a challenge.

To date, there have been some high-impact review papers on the grain refinement of light alloys [1,3,4,10,11], on the basis of which some basic aspects of the effect of grain refinement with Zr on Mg alloys can be found. However, most of the information from the references is so fragmented that readers must browse through more papers to acquire sufficient knowledge. In other words, there is still a lack of a systematic review on the effect of grain refinement with Zr on Mg alloys. Considering the importance of Zr refinement, this paper comprehensively summarizes the recent advances in effect of grain refinement with Zr on Mg alloys. The principal text includes the alloying process of Zr, the mechanism of grain refinement with Zr, factors influencing the grain refinement behaviors of Zr, methods to improve grain refinement efficiency of Zr, and prospective research on Zr grain refinement. This review will provide researchers and engineers with a full understanding of Zr grain refinement in Mg alloys.

## 2. Alloying Process of Zr

### 2.1. The Methods of Zr addition

The direct addition of pure Zr metal into Mg melt is very difficult, because Zr has a much higher melting point (~1852 °C) than Mg (~650 °C) and a stable oxide film that normally presents on Zr particle surfaces [9,12]. Before the popular use of the Mg-Zr master alloy, many approaches were tried, such as alloying with pure Zr powder, ZrO<sub>2</sub>, or Zr-rich salt mixtures [6,13–15]. Table 1 shows some examples of early patents claiming methods for alloying Zr in Mg alloy melt [16–19]. For example, Sauerwald et al. tried using the Zr powder as a source [16]. However, Zr powder is prone to ignite, and the oxide film inhibits the diffusion of Zr in the Mg melt. In addition, the direct addition of Zr-containing chloride or fluoride salt mixtures into Mg alloy melt has also been tried, which showed that the residuals MgCl<sub>2</sub> or MgF<sub>2</sub> are difficult to remove from the melt [6]. In a word, early methods were not satisfactory due to their complicated processes and the contamination of the melt. Recent research has attempted the traditional Zr-rich salts method again, through the addition of K<sub>2</sub>ZrF<sub>6</sub>-NaCl-KCl [20,21], KZrF<sub>5</sub>-LiCl-KCl-CaF<sub>2</sub> [22] or ZrCl<sub>4</sub> [23] salts to Mg-RE alloys, further confirming that good grain refinement effects can be achieved. Nevertheless, the salt inclusions are really difficult to remove.

**Table 1.** Early patents of Zr alloying methods in Mg alloy.

Ref.	Composition or Route	Aim
[16]	Pure Zr powders + Mg melt at 700 °C → solidified → annealed at about 600 °C for 4–5 days → Mg-Zr master alloy	Preparing Mg-Zr master alloy
[17]	ZrCl <sub>4</sub> (15~60%) + KCl (≥10%) + BaCl <sub>2</sub> (≥30%)	Preparing Zr-rich salts mixture used in Mg melt
[18]	ZrCl <sub>4</sub> (5~25%) + ZrO <sub>2</sub> (≤25%) + KF + BaCl <sub>2</sub> . ZrO <sub>2</sub> as inspissation agent	
[19]	ZrCl <sub>4</sub> (33~45%) + KCl (33~45%) + MnCl <sub>2</sub> (12~33%) + BaCl <sub>2</sub> (≤20%)	

In addition to the direct use of Zr-rich salt mixtures, earlier researchers have also tried to prepare a Mg-Zr master alloy. For example, Robert [24] tried three different routes to produce Mg-Zr master alloys: (1) Distillation of Mg out of low-Zr Mg-Zr alloy to obtain a high-Zr Mg-Zr alloy. Mg could either be sublimated at pressures of mercury below about 3 mm, or boiled at higher pressures. However, the alloys showed serious compositional segregation. (2) Fusing compacts of ZrH<sub>2</sub> powder and Mg shavings. The reason ZrH<sub>2</sub> was used is that ZrH<sub>2</sub> is not pyrophoric, unlike pure Zr powder. A compact of ZrH<sub>2</sub> powder and Mg shavings was formed using a hydraulic press. Then, the compact was heated to a temperature above 900 °C for a couple of hours in an electric vacuum furnace in order to remove the H<sub>2</sub> and form Mg-Zr alloy. However, several trials only demonstrated limited success. (3) Melting compacts of Zr and Mg shavings in a sealed steel “bomb”. The steel bomb was heated in an electric muffle furnace at a temperature below 500 °C for a couple of

hours. After being taken out of the furnace, it was shaken vigorously and then quenched in water. The results showed that the Mg-Zr alloy was of sufficient quality. However, due to their complex processes and low production capacity, these methods have been abandoned.

In terms of the development of a production method for Mg-Zr master alloys, the chemical reduction of Zr-rich fluoride or chloride salt with molten Mg has become a suitable route [14]. During the production process of the Mg-Zr master alloy, the Zr particles were formed in-situ within the Mg matrix, and thus the particle surfaces were not contaminated with O<sub>2</sub> or other impurities. This kind of Zr particle is clean, active, and quickly diluted in Mg melt, helping to easily achieve the saturation of Zr content [6]. Therefore, since about 1960, only Mg-Zr master alloy has been widely used as a satisfactory Zr refiner in Mg alloys. A famous commercial Mg-Zr product named Zirmax, developed by Magnesium Elektron in the UK, has become one of the popular products [6]. This product contains nominally more than 30% Zr in a relatively homogeneous distribution of Zr particles.

## 2.2. The Features of the Mg-Zr master Alloy

Generally, Mg-Zr master alloy contains a large number of Zr particles, the sizes of which range from the sub-micron level to hundreds of microns. The backscattered electron (BSE) scanning electron microscopy (SEM) images in Figure 1 show the typical microstructural features of different Mg-Zr products available on the market [25–27]. It can be seen that the Zr sizes exhibit a log-normal distribution. However, the number density of each size range has great differences, depending on the preparation parameters.

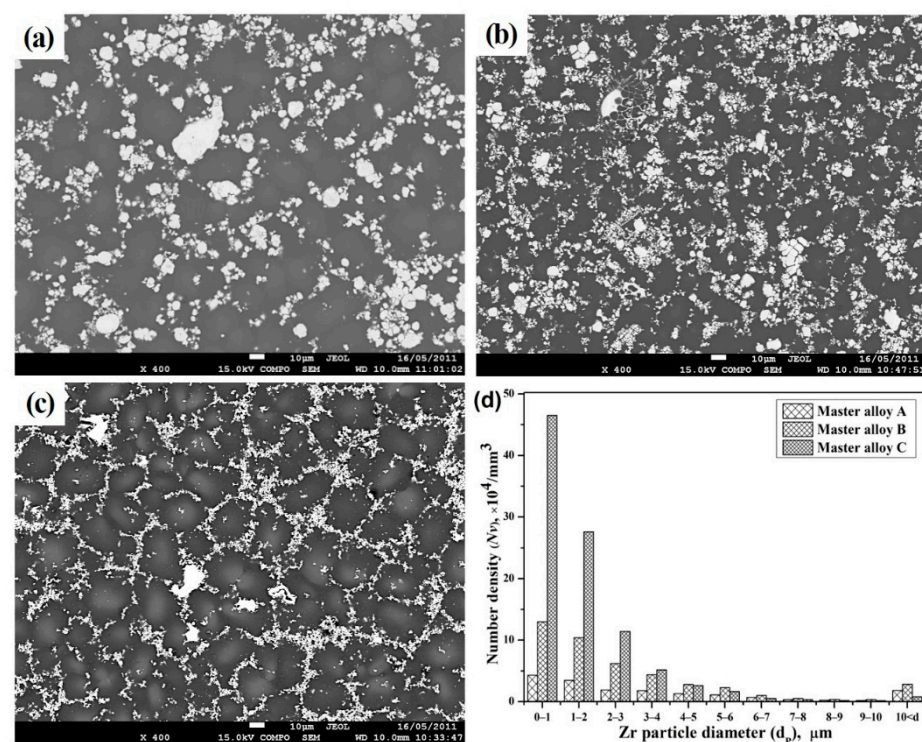


**Figure 1.** SEM backscattered electron (BSE) images of different Mg-Zr master alloys [25]: (a) Mg-30 wt.% Zr; (b) Zirmax<sup>®</sup> Mg-33% Zr, (c) AM-CAST<sup>®</sup> Mg-25 wt.% Zr; and (d) Zr particle size distributions [26]. Reprinted with permission from ref. [26]. Copyright 2013 Wiley.

To ensure the high absorptivity of Zr in Mg melt, some aspects should be considered, such as excessive addition of Zr, high alloying temperature, and adequate stirring. In particular, high temperature and adequate stirring accelerate the dissolution of Zr [28]. With the aid of stirring, the dissolution of Zr can be completed within a few minutes in the temperature range 730–780 °C [29]. However, if the temperature is above 780 °C, the difficulties in melt protection obviously increase, since Mg melt is prone to oxidation and

burning, although protective gas (e.g.,  $\text{CO}_2 + \text{SF}_6$ ) can be used. Normally, in industrial practice, temperatures below  $780\text{ }^\circ\text{C}$  are regarded as suitable for Zr alloying.

### 2.3. Settling Behavior of Zr Particles during Alloying

The settling of Zr particles, forming sediment, is the most serious problem during Zr alloying process. This is due to their having a higher density ( $\sim 6.52\text{ g/cm}^3$ ) than liquid Mg ( $\sim 1.7\text{ g/cm}^3$ ), leading to the spontaneous settling of Zr particles. The bigger the Zr particle size is within the Mg-Zr master alloy, the faster the rate of settling will be. The settling of Zr reduces the absorption of Zr, causes waste of Zr, and forms a non-uniform microstructure from the top to the bottom of the ingot [3,30]. To compensate for the loss of Zr, the addition of Zr is always as high as 1~3 wt.% in practical operations, which is 2~4 times the nominal Zr composition of Mg alloys [29,31]. Therefore, the expensive Zr waste increases the cost of the Mg alloy.

Figure 2a,b show the experiment and simulation results, respectively, of Zr settling reported by Qian [30]. The settling behavior of Zr particles follows the Stokes law:

$$S \approx \frac{g(\rho_{\text{Zr}} - \rho_{\text{Mg}})d_p^2 t}{18\eta_{\text{Mg}}} \quad (1)$$

where  $S$  is settling distance,  $g$  is gravitational acceleration,  $\rho_{\text{Zr}}$  is the density of Zr,  $\rho_{\text{Mg}}$  is the density of Mg melt,  $\eta_{\text{Mg}}$  is the viscosity of Mg melt,  $d_p$  is the diameter of Zr particle, and  $t$  is the holding time. It can be seen that larger Zr particles settle more quickly than smaller ones;  $S$  increases with prolonging time; a higher melt temperature favors quicker settling due to the lower viscosity of Mg melt. These results can guide the industrial operations of the Zr alloying process in order to avoid severe loss of Zr. Generally, the melt should be cast after settling for 15~30 min, in order to prevent continuous settling and the fading of the grain refinement. Moreover, after setting for more than 60 min, the melt can be re-stirred to recover the settled Zr particles [29,32], which makes the casting process more complicated.

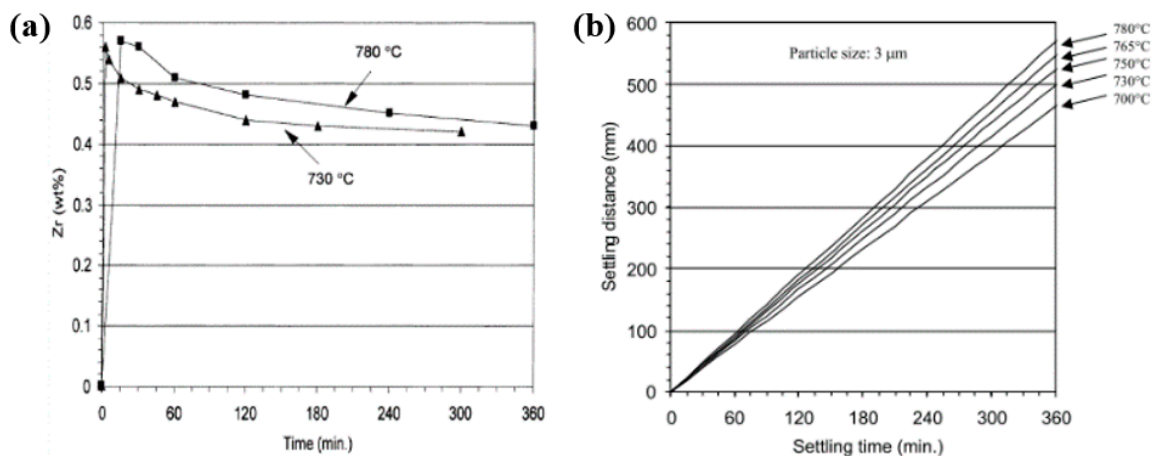


**Figure 2.** (a) Experimental results for settling; (b) predicted settling results of  $3\text{ }\mu\text{m}$  Zr particles in pure Mg melt as a function of time and temperature [30]. Reprinted with permission from ref. [30]. Copyright 2001 Elsevier.

Recently, to avoid the settling problem and reduce costs, the in-situ  $\text{Al}_2\text{RE}$  nucleating particles were trialed to replace Zr [33–35]. The grain refinement effect of  $\text{Al}_2\text{RE}$  is comparable to that of Zr. However, the aging precipitation ability is reduced due to the consumption of RE element following the addition of Al, and the formation of needle-like  $\text{Al}_x\text{RE}_y$  phases is detrimental to the mechanical properties.

### 3. Grain Refinement Mechanisms of Zr

It is generally accepted that the grain refinement mechanism of Zr is dictated by both soluble and insoluble Zr. With the help of quantitative analysis of  $Zr_S$  and  $Zr_T$ , the grain refinement behaviors of Zr can be well estimated [36]. On the one hand, when the Zr content reaches the peritectic point, the peritectic reaction is believed to be the core mechanism of grain refinement [3,4,31,37,38]. On the other hand, a grain refinement effect can also be observed when the Zr content is far below the peritectic point, which is thought to be due to the constitutional supercooling (CS) effect generated by soluble Zr [3,4,31,37,38]. This section will briefly discuss these two aspects.

#### 3.1. Nucleation Effect

##### 3.1.1. Peritectic Reaction

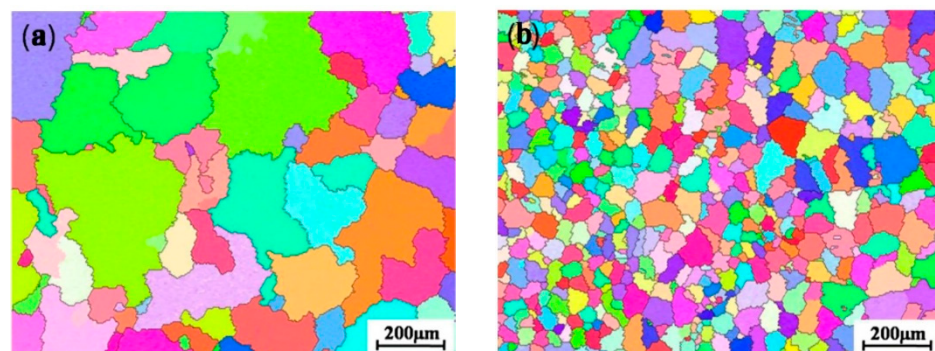
According to Mg-Zr binary phase diagram, Zr and Mg do not form compounds, and there is a peritectic reaction at 653.5 °C. The peritectic reaction leads to Mg nucleation at the primary Zr-rich sites, which plays a very important role in the grain refinement process of Mg by Zr [10,13,39]. The peritectic point of Zr composition was previously found to be 0.6% Zr. However, re-assessment shows that it is substantially lower, at about 0.45% [4]. Thus, it is possible to use a smaller amount of Zr, thus reducing the cost of grain refinement [40].

Table 2 presents a comparison between the crystal structures of Mg and Zr, indicating that both  $\alpha$ -Zr and  $\alpha$ -Mg have HCP crystal structures, and their lattice parameters are quite similar. Thus, Zr has outstanding potency for acting as a nucleation substrate for Mg phase [41]. The perfect nucleation ability of Zr can be further verified by low undercooling ( $\Delta T_n \approx 0.15$  °C [42]) equal to that for Al grains nucleating on  $TiB_2$  substrates ( $\sim 0.2$  °C [43]).

**Table 2.** The crystal structure and lattice parameters of Mg and Zr [41].

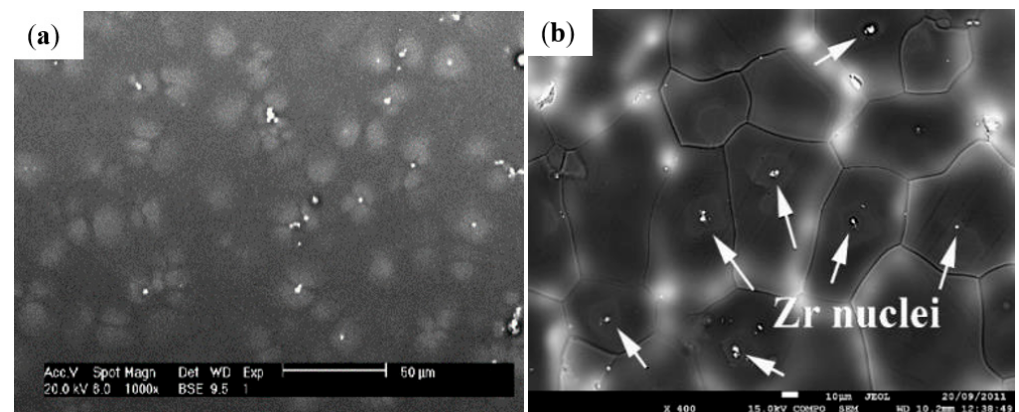
Phase	Crystal Structure	Lattice Parameters
$\alpha$ -Mg	HCP	$a = 0.320$ nm, $c = 0.520$ nm
$\alpha$ -Zr	HCP	$a = 0.323$ nm, $c = 0.514$ nm

Figure 3 shows an example demonstrating that 0.5% Zr content can strongly refine the grains of Mg alloy, where the grain size of WE54 Mg alloy (Mg-5Y-4HRE-0.5Zr, HRE = heavy rare earth elements) was refined from 295  $\mu$ m to 83  $\mu$ m [44] under the conditions of pouring at about 780 °C into a steel mold preheated to 300 °C. This content of Zr is basically in accordance with the peritectic point in the Mg-Zr phase diagram. The simulation work performed by Zhao et al. [45] further showed that the growth velocity of dendrite tip of Mg-4Y alloy can be reduced to be one-sixth (1/6) using 0.5Zr, forming a fine grain size. However, this perspective still requires further evidence.



**Figure 3.** An example showing the powerful effect of grain refinement with Zr on Mg alloy. Electron backscattered diffraction technology (EBSD) image of: (a) Zr-free WE54 alloy; (b) Zr-containing WE54 alloy. Poured at 780 °C into a steel mold (300 °C). Reprinted with permission from ref. [44]. Copyright 2013 Elsevier.

In early work, it was thought that only the dissolved Zr was effective for grain refinement, because saturated dissolved Zr content meets the standards of a peritectic composition. However, later work verified that Mg grains can nucleate not only onto Zr particles precipitating from the melt during cooling, but also onto undissolved Zr particles through heterogeneous nucleation [4,31,38,46]. The products of peritectic solidification in the microstructure of Zr-containing Mg alloy are Zr-rich halos or cores, present in most Mg grains, as shown in Figure 4 [26,37]. The Zr-rich halo shows either dendritic or nearly spherical growth, depending on the soluble Zr content. A higher level of soluble Zr (close to the solubility) usually leads to spherical halo, while a lower level of soluble Zr leads to a dendritic halo [38].



**Figure 4.** SEM BSE image of Zr-rich cores in: (a) Mg-0.56Zr alloy [37]; Reprinted with permission from ref. [37]. Copyright 2002 Elsevier. (b) Mg-5Gd-1.5Y-0.55Zr alloy [26]; Reprinted with permission from ref. [44]. Copyright 2013 Wiley.

### 3.1.2. HRTEM Observations of Zr Nucleus

To facilitate the understanding of the grain refinement mechanism, the orientation relationships (ORs) between Mg grains and Zr nuclei were observed via high-resolution transmission electron microscopy (HRTEM). Table 3 summarizes some of the reported coherent or semi-coherent ORs in grain-refined Mg alloys [23,47–51]. All the ORs have low misfits, which are responsible for the good nucleating potency of Zr. For example, the misfit of OR  $[\bar{1}2\bar{1}3]_{Mg} \parallel [\bar{1}2\bar{1}3]_{Zr} + (1\bar{1}2)_{Mg} \wedge (1\bar{1}2)_{Zr}$ , OR  $[2\bar{1}\bar{1}0]_{Mg} \parallel [2\bar{1}\bar{1}0]_{Zr} + (0001)_{Mg} \parallel (0001)_{Zr}$  and OR  $[01\bar{1}1]_{Mg} \parallel [01\bar{1}1]_{Zr} + (\bar{1}011)_{Mg} \parallel (\bar{1}011)_{Zr}$  is only 0.13% [47], 0.9% [49] and 0.41% [50], respectively. Figure 5 shows a typical example of OR  $[2\bar{1}\bar{1}0]_{Mg} \parallel [2\bar{1}\bar{1}0]_{Zr} + (01\bar{1}\bar{1})_{Mg} \parallel (01\bar{1}\bar{1})_{Zr}$  observed in the sand-cast Mg-8Gd-3Y-0.82Zr alloy [23].

**Table 3.** Reported ORs between Mg and Zr in grain-refined Mg alloys<sup>1</sup>.

ORs	Alloys	Processing	Ref.
$[2\bar{1}\bar{1}0]_{Mg} \parallel [2\bar{1}\bar{1}0]_{Zr} + (01\bar{1}\bar{1})_{Mg} \parallel (01\bar{1}\bar{1})_{Zr}$	Mg-7.43Gd-2.74Y-0.82Zr	Sand-cast	[23]
$[\bar{1}2\bar{1}3]_{Mg} \parallel [\bar{1}2\bar{1}3]_{Zr} + (11\bar{2}2)_{Mg} \wedge (11\bar{2}2)_{Zr}$	Mg-0.5Zr	Gravity cast	[47]
$[\bar{1}2\bar{1}3]_{Mg} \parallel [\bar{1}2\bar{1}3]_{Zr} + (10\bar{1}0)_{Mg} \parallel (10\bar{1}0)_{Zr}$	Mg-1.0Zr	Gravity cast	[47]
$[2\bar{1}\bar{1}0]_{Mg} \parallel [2\bar{1}\bar{1}0]_{Zr} + (0001)_{Mg} \parallel (0001)_{Zr}$	Mg-0.5Zr	Gravity cast	[48]
	Mg-1.0Zr	IMS + Gravity cast	[49]
$[01\bar{1}1]_{Mg} \parallel [01\bar{1}1]_{Zr} + (\bar{1}011)_{Mg} \parallel (\bar{1}011)_{Zr}$	Mg-1.0Zr	HPDC	[50]
$[24\bar{2}3]_{Mg} \parallel [24\bar{2}3]_{Zr} + (10\bar{1}0)_{Mg} \parallel (10\bar{1}0)_{Zr}$	Mg-0.1Zr	HPDC	[51]
	Mg-0.52Zr	Gravity cast	[27]

<sup>1</sup> In Table 3,  $\wedge$ —tilted directions;  $\parallel$ —parallel directions; IMS—intensive melt shearing; HPDC—high-pressure die casting.

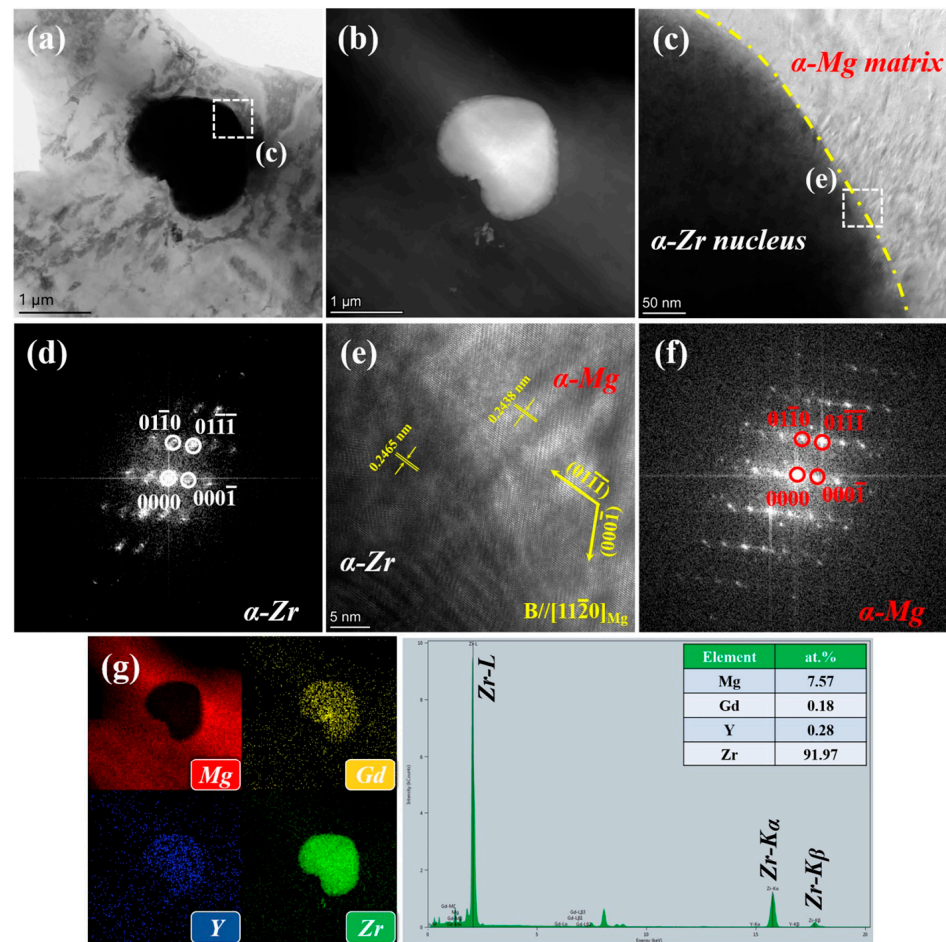


**Figure 5.** TEM showing OR between Mg matrix and Zr nucleus in Mg-8Gd-3Y-0.82Zr alloy: (a) bright-field image; (b) dark-field image; (c) enlarged view of the selected area in (a); (e) HRTEM image of the interface between Mg matrix and Zr nucleus (beam  $\parallel [2\bar{1}\bar{1}0]_{Zr}$ ); (d,f) fast Fourier transform (FFT) spectrum of  $\alpha$ -Zr and  $\alpha$ -Mg, respectively; (g) EDS analysis of Zr nucleus. Reprinted with permission from ref. [23]. Copyright 2021 Elsevier.

With the analysis of HRTEM and the selected area diffraction pattern (SADP), Saha concluded that Mg grains only nucleate on the “faceted” crystal planes of Zr particles [47,48], e.g., the basal planes  $\{0001\}$  or the prismatic planes  $\{10\bar{1}0\}$ . However, contradicting Saha, Peng et al. [49] found that the interface between the Zr nucleus and the Mg matrix was “curved” rather than “faceted”. The curved interface, in combination with coherent ORs, provides perfect lattice matching along various directions and across various planes, benefitting the nucleation of Mg grains on the Zr particle surface.

Although various ORs have been reported, as shown in Table 3, Yang et al. [51] suggested that very strict ORs are not required for Zr nuclei, because Zr particles may be wetted by Mg melt on all exposed crystal planes. This viewpoint was validated by HRTEM observations in Ref. [49], as shown in Figure 6 [51]. Perfect coherent ORs can be observed, among which even the slightly higher index OR  $[2\bar{4}2\bar{3}]_{Mg} \parallel [2\bar{4}2\bar{3}]_{Zr} + (10\bar{1}0)_{Mg} \parallel (10\bar{1}0)_{Zr}$  is present, which is similar to that described in Ref. [27]. Thus,  $\alpha$ -Mg grains can grow epitaxially on any suitable planes of Zr nuclei. Recently, in-situ neutron diffraction observations have provided further evidence of the grain refinement mechanism of Zr, showing that with the addition of Zr, all of the diffraction intensities of the  $(10\bar{1}0)$ ,  $(0002)$  and  $(10\bar{1}1)$  planes of Mg-5Zn-0.7Zr alloy increase at similar rates during the early stages of solidification, leading to the formation of a uniform grain structure [52].

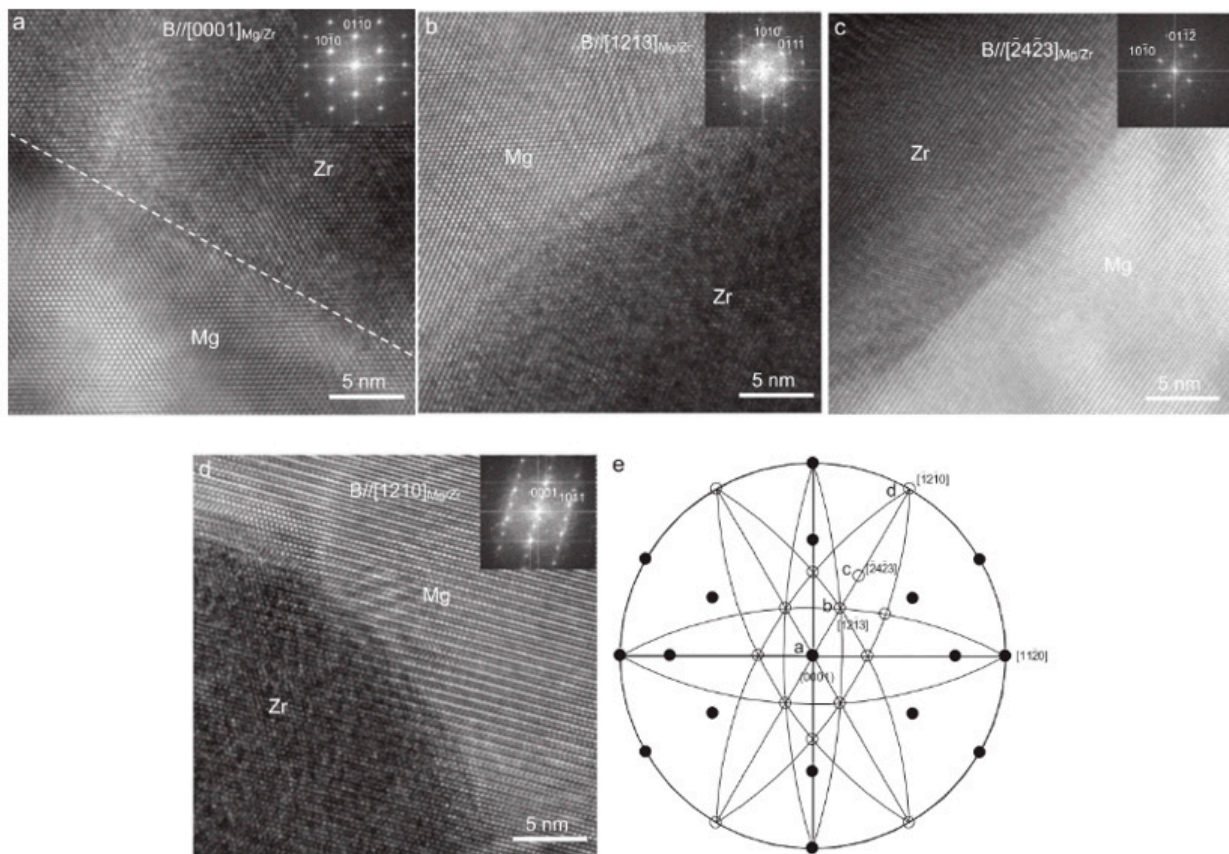


**Figure 6.** HRTEM images showing: (a) faceted interface; (b–d) curved interfaces between  $\alpha$ -Mg grains and Zr nuclei in Mg-0.1Zr alloy along four different low-index zone axes. (e) Stereographic projection of HCP structure showing the various ORs (a–d) within a  $90^\circ$  range [51]. Reprinted with permission from ref. [51]. Copyright 2015 Elsevier.

### 3.2. Constitutional Supercooling (CS) Effect

Zr can affect both the nucleation and the growth of the dendritic phase in Mg alloy depending on its status in the melt [53]. When the addition of Zr content is higher, grain refinement can be achieved due to the large number of Zr nucleating particles. When the addition of Zr is low, an obvious grain refinement effect can still be observed. This is mainly due to the strong CS effect of solute [4,10,26,43,54–56], since Zr is also a solute element in the Mg-Zr system. The growth restriction factor (*GRF*, *Q*) is defined as follows to reflect the CS effect [4,43,54]:

$$Q = m(k-1) \quad (2)$$

where *m* is the liquidus gradient and *k* is the partition coefficient. The larger the *Q* value is (unit K or  $^\circ\text{C}$ ), the stronger the grain refinement effect will be. On the basis of phase diagram analysis, the *Q* value of Zr was calculated to be 38.29, which is much higher than that of most of the alloying elements, such as Al (4.32), Y (1.70), Zn (5.31), etc. [4,11], indicating that soluble Zr produces a strong grain refinement effect [1,4]. Peng et al. [57] proved that the grain refinement of Mg-9Gd-3Y-0.25Zr alloy (low Zr) was mainly contributed by the *GRF* effect, while the grain refinement of Mg-9Gd-3Y-0.51Zr alloy (high Zr) was mainly contributed by the heterogeneous nucleation of Zr particles. The CS effect of Zr was recently verified by Zhang et al. [57]. As shown in Figure 7, remarkable grain refinement (from  $74 \mu\text{m}$  to  $3.5 \mu\text{m}$ ) occurred in the melt pool of the laser-surface-remelted (LSR) Mg-3Nd-1Gd-0.5Zr alloy, which was mostly due to the high CS effect of soluble Zr caused by LSR.

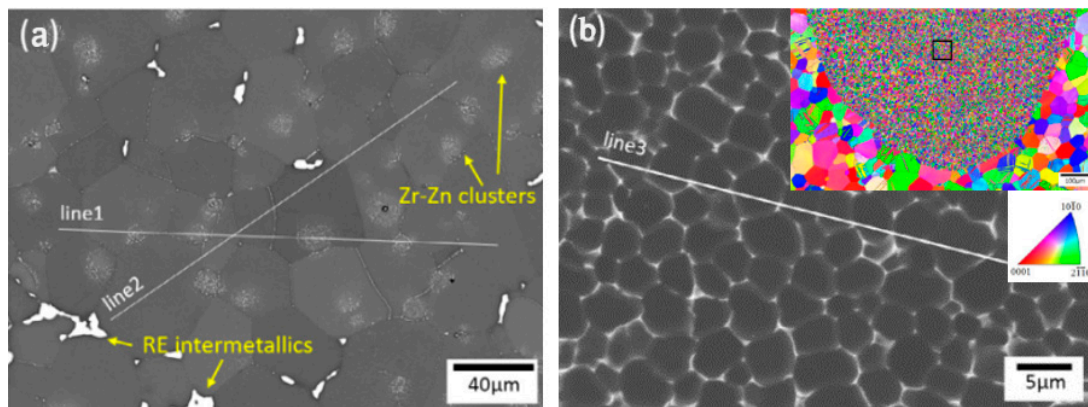


**Figure 7.** SEM BSE images of the laser-remelted Mg-3Nd-1Gd-0.5Zr alloy showing the microstructure of: (a) the substrate; (b) the melt pool, the cross-section EBSD analysis of which is included as an inset in the upper-right corner [58]. Reprinted with permission from ref. [58]. Copyright 2020 Elsevier.

In summary, the nucleation effect combined with the CS effect leads to a high nucleation rate and low undercooling, resulting in the powerful effect of grain refinement with Zr. Such effects are not only of benefit to achieving equiaxed grains during the casting process, they also facilitate the formation of slurries with fine and spherical primary particles during the semi-solid forming process [59,60].

#### 4. Factors Influencing the Grain Refinement Behaviors of Zr

This section briefly summarizes the effects that influence the Zr alloying efficiency during the melting process.

##### 4.1. Effect of Zr Size Distribution in Mg-Zr Master Alloy

In the microstructure of Mg alloy refined by Zr, Qian et al. [30,61] observed that the majority of Zr nuclei had sizes in the range of 1~5 µm. Sun et al. [25–27] further systematically compared the size distribution of different Mg-Zr master alloys (Figure 1) and the subsequent grain refinement efficiency on Mg-Gd-Y alloys (Figure 8). It was found that Mg-Zr master alloys with more Zr particles within the size range 1~5 µm (i.e., master alloy C) exhibited better grain refinement efficiency. This is because both the saturation of soluble Zr content and a greater number of Zr nucleation sites could be achieved when the Mg-Zr master alloy had a finer Zr particle distribution.

##### 4.2. Effect of Cooling Condition

Generally, increasing the cooling rate ( $\dot{T}$ ) results in a decrease in grain size. For example, Liu et al. [62] showed that the grain size of Mg-Zr binary alloys (0.3, 0.7 or 1.2Zr) decreased with increasing cooling rate from sand mold to Cu mold. Sun et al. [63] found that the relationship between the grain size of Mg-Y-Zr alloy (1~9Y, 0.1~0.5Zr) and  $1/\sqrt{Q\dot{T}}$  could be linearly fitted at a cooling rate  $\leq 80$  °C/s (Figure 9 shows Mg-1Y-Zr alloy as an example of this phenomenon). Yang et al. [51] showed that, compared with traditional gravity casting, HPDC improved the percentage of activated Zr nuclei from 1~2% to 48.78% in the Mg-0.1Zr alloy, and resulting in finer grains.

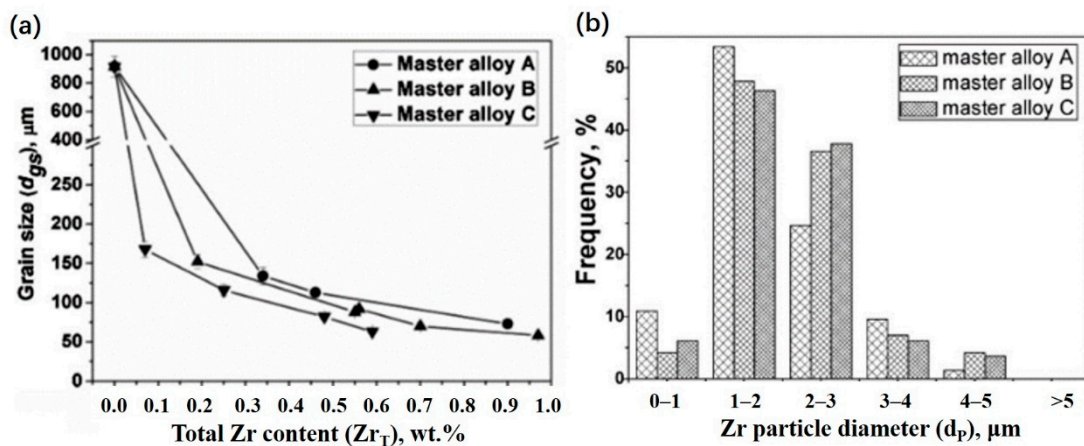


**Figure 8.** (a) The relationship between grain size ( $d_{gs}$ ) and total Zr content ( $Zr_T$ ) for Mg-5Gd-1.5Y alloy refined using different Mg-Zr master alloys. (b) The distribution of Zr nuclei in Mg-5Gd-1.5Y alloy with  $Zr_T$  contents of 0.46, 0.55 and 0.59, inoculated by master alloys A, B and C, respectively [26]. The microstructure and Zr particle size distributions of the Mg-Zr master alloys are shown in Figure 1. Reprinted with permission from ref. [26]. Copyright 2013 Wiley.

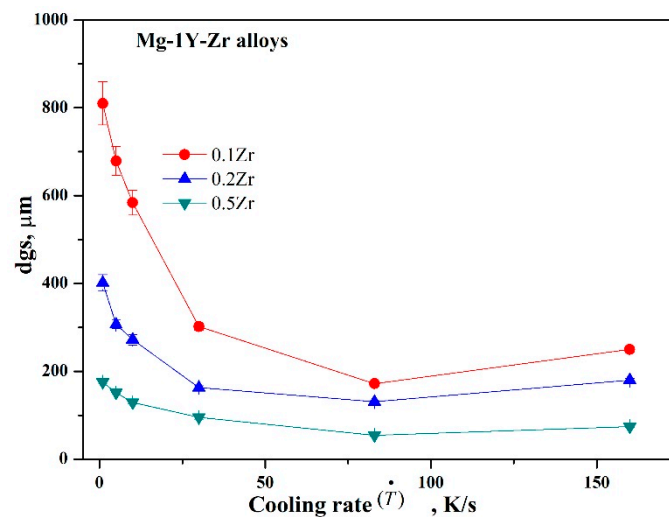


**Figure 9.** Effect of cooling rate ( $\dot{T}$ ) on the grain size ( $d_{gs}$ ) of Mg-1Y-Zr alloy [63]. Reprinted with permission from ref. [63]. Copyright 2020 Springer.

Nevertheless, grain coarsening has also been observed under some cases of high cooling rate and steep thermal gradient [58,63]. According to Figure 9, by Sun et al. [63], grain coarsening of the Mg-Y-Zr alloy (1~9Y, 0~0.5Zr) occurred at a cooling rate 160 °C/s (with rapid water-quenching). This was due to the reduction in size of the CS zone, decreasing the likelihood of further nucleation. Yang et al. [50] showed that the grain coarsening effect occurred in HPDC Mg-1Zr alloy, in contrast to HPDC pure Mg. The grain size increased abnormally from 6.7 to 18.9  $\mu\text{m}$  following the addition of 1% Zr. This change was attributed to the competition between the native MgO and the Zr particles. Without the addition of Zr, the high number density of the in-situ MgO particles permitted them to act as nucleation sites, due to a the low misfit with Mg (5.46%), leading to a finer grain size. However, with the addition of Zr, the Zr particles acted as nucleation sites first, thereby suppressing the activation of the in-situ MgO particles. More importantly, the number density of the Zr particles was lower than that of the in-situ MgO particles. Therefore, the grain size of Mg-1Zr was coarser than that of pure Mg.

### 4.3. Effect of Alloying Elements

Contrary effects can be found depending on the elements employed. On the one hand, the elements Al [64,65], Mn, Si, Fe [29,66], Sn, Ni, Co and Sb [29] inhibit the grain refinement ability of Zr, which is referred to as the poisoning effect. This is mainly due to the reactions with Zr forming stable compounds that can no longer act as a nucleant [4,13,29]. Beryllium (Be) also poisons Zr, but via a different mechanism, which is probably the formation of a new coating on the Zr particle surface, thus reducing the potency of the Zr [67]. On the other hand, the elements Ca [68] and Zn [69–71] enhance the grain refinement ability of Zr, mainly via the mechanism increasing the soluble Zr content. This section summarizes the effects of these elements.

#### 4.3.1. Al

Al poisons the effect of grain refinement with Zr, which is the main reason for which Mg-Al alloy cannot be grain-refined using Zr. Tamura et al. [72] found that even the trace addition of 0.015% Zr could severely coarsen the grain size of high-purity Mg-9Al alloy; Kabirian et al. [64] found that the dendrites of AZ91 alloy were greatly coarsened by the addition of 0.2~1.0% Zr; Balasubramani et al. [65] found the grain size of Mg-1Zr was sharply coarsened from  $114 \pm 38 \mu\text{m}$  to  $1550 \pm 38 \mu\text{m}$  with the addition of 0.2% Al (Figure 10). Two reasons have been proposed. One is that Zr poisons the surface of the native Al-carbide nuclei (such as  $\text{Al}_4\text{C}_3$  [73]) that are originally present in high-purity Mg-9Al alloy. Another is that the consumption of solute Al by Zr (or solute Zr by Al) reduces the extent of the CS effect. The Al-Zr compounds were identified to be  $\text{Al}_2\text{Zr}$  [64],  $\text{Al}_3\text{Zr}_2$  [64] or  $\text{Al}_3\text{Zr}$  [65]. Despite the negative effect on grain refinement, Al-Zr compounds can increase the thermal stabilities of grain during heat treatment, refine grains during hot deformation [74], and increase creep resistance [75].

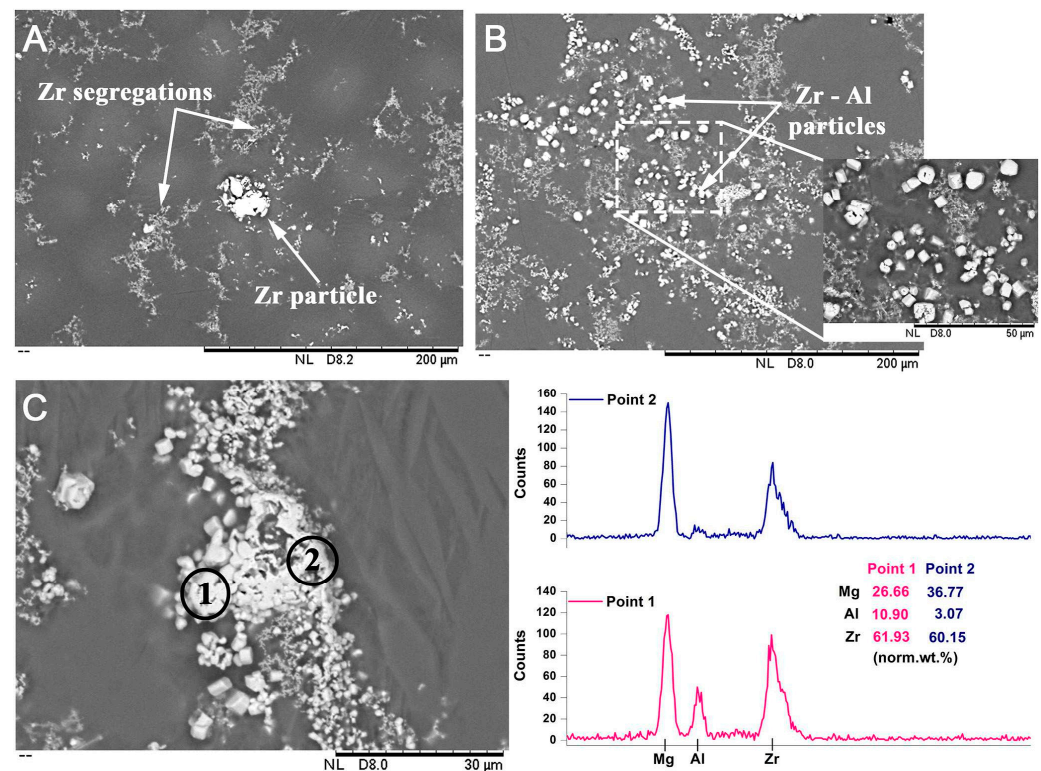


**Figure 10.** SEM BSE images showing: (A) blocky Zr particles and fine Zr particles in Mg-1Zr alloy; (B) faceted  $\text{Zr}_x\text{Al}_y$  particles in Mg-1Zr-Al-Be alloy; (C) Zr clusters surrounded by fine precipitates of  $\text{Zr}_x\text{Al}_y$  particles in Mg-1Zr-Al-Be alloy, EDS testing point 1 is rich in Al and Zr, whereas point 2 is rich in Zr. The samples were cut from the bottom of an ingot to observe the clusters [65]. Reprinted with permission from ref. [65]. Copyright 2004 Elsevier.

#### 4.3.2. Fe

Fe is one of the most common impurities in Mg alloys, and may result from the raw materials, fluxes, crucible, and stirring tools used. Fe is detrimental to the effect of grain refinement with Zr. This can be understood from two perspectives.

On the one hand, Fe can react with Zr in the Mg melt, forming the compound  $\text{Fe}_2\text{Zr}$ , as verified by Cao et al. [66]. As a result, the Zr content is rapidly consumed, and the grain refinement effect is remarkably reduced. This effect has also been observed during the remelting process of pre-alloyed or commercial ingots of Zr-bearing Mg alloys when using an Fe crucible. An obvious loss of dissolved Zr takes place due to the diffusion of Fe through the Mg melt, finally leading to the addition of extra Zr in order to achieve the required level of grain refinement [76].

On the other hand, trace Fe and Si impurities on tiny Zr particles may alter the surface chemistry of the Zr particles, upsetting the coherent match between the Zr and Mg lattices, as reported Davis et al. [77]. Therefore, the nucleating potency of the Zr particles is decreased, reducing the grain refinement effect.

On the basis of these analyses, it can be seen that when an Fe crucible and Fe stirring paddle are used during melting of Mg alloys, a protective coating (e.g., BN coating [66]) should be pre-coated to inhibit the dissolution of Fe into the Mg melt. However, it has been reported that, by taking advantage of the effective removal of Fe by Zr, high-purity Mg alloys containing less than 1 ppm Fe can be produced [78].

#### 4.3.3. Be

Cao et al. [67] investigated the effect of trace addition of Be on the grain refinement of Mg-0.5Zr alloy, as shown in Figure 11, where a significant grain coarsening effect can be observed. However, since Be was added in the form of Al-5Be master alloy, the influence of the consumption of Zr by Al cannot be neglected. Thus, the alloys were designed in two groups, i.e., a low-Zr-content group (ZM1~ZM4) and a high-Zr-content group (ZM5). It can be seen that with increasing addition Be from 10 to 100 ppm, the grain size of ZM1~ZM4 increased gradually, which was mainly because of the continuous consumption of Zr by Al. Nevertheless, with the further addition of 0.5% Zr (ZM5), the grain size continued to coarsen, rather than recovering. Therefore, a poisoning effect of Be was deduced, whereby Be, as a surface-active ‘surfactant’, readily coats the surfaces of heterogeneous nucleant particles such as Zr particles or native particles (Fe-rich, carbon-rich nuclei) destroying the nucleating potency.

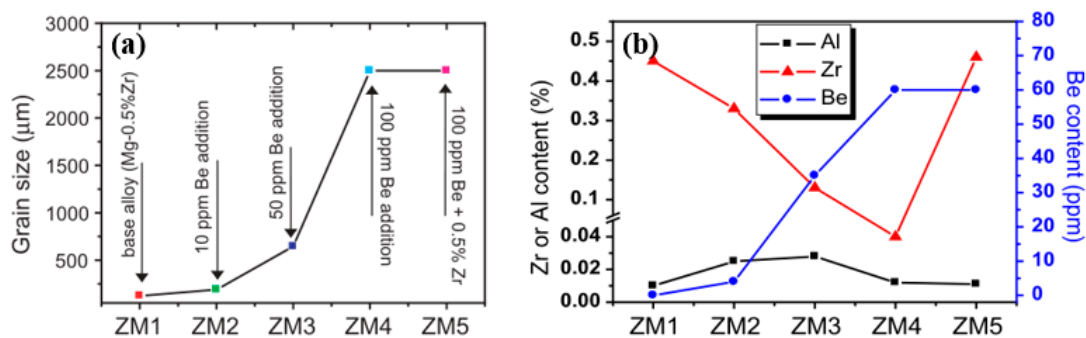


**Figure 11.** (a) Grain size as a function of Be addition. (b) Be, Al and Zr contents in alloys. ZM1: base alloy Mg-0.5% Zr; ZM2: 10 ppm Be addition; ZM3: 50 ppm Be addition; ZM4: 100 ppm Be addition; ZM5: 100 ppm Be + 0.5% Zr. [67]. Reprinted with permission from ref. [67]. Copyright 2004 Elsevier.

#### 4.3.4. Ca

Chang et al. [68] showed that the grain size of squeeze-cast Mg- $x$ Ca-0.6Zr ( $x = 0.2\sim 1.2$ ) alloy was finer than that of squeeze-cast Mg-0.6Zr alloy. They concluded that Ca was able to increase the effect of grain refinement with Zr. The reason for this was explained from a thermodynamics perspective. Before the addition of Ca, the Mg melt reacts preferentially

with O<sub>2</sub>, forming MgO inclusions that envelope the Zr particles. This effect increases the difficulty of the dissolution of Zr. After the addition of Ca, the formation of MgO is suppressed due to CaO possessing a lower standard free energy than MgO. Accordingly, the dissolution of Zr particles becomes more efficient, and the interface wettability between Zr particles and the Mg matrix improved. Therefore, the combined addition of Zr and Ca shows a better grain refinement effect.

However, the effect of CS was neglected in [68]. According to StJohn et al. [4], the GRF value for Ca is 11.94, which is the third highest among all solute elements in Mg alloy (the first is Fe, at 52.56, and the second, Zr, at 38.29). Thus, the high GRF of Ca may be another reason for the increase in the grain refinement effect of Mg-Ca-Zr alloy.

#### 4.3.5. Zn

Zn has been reported to show contradictory influences on the effect of grain refinement with Zr in Mg-Zn-Zr alloy, depending on the Zn content. According to Hildebrand et al. [69] and Li et al. [70], there exists a critical Zn content (3~4%) below which the grain size is gradually refined, but beyond which the grain size coarsened. The reasons for this have been well explained. When Zn content does not exceed 3~4%, the soluble Zr content increases with increasing Zn content, resulting in a finer grain size [69]. When Zn content exceeds 4%, Zn and Zr form the stable compounds ZnZr<sub>2</sub> or Zn<sub>2</sub>Zr<sub>3</sub> [79], decreasing the soluble Zr content and resulting in a coarser grain size. However, in partial divergence from Hildebrand et al. [69], Li et al. [70] attributed the grain coarsening effect at higher Zn contents to the “dendrite coherency theory”. A large constitutional undercooling caused by higher Zn content leads to instability of the S-L interface. The sharp tip of the dendrite increases the growth rate of the dendritic grains, thus leading to coarser grains.

In addition, higher Zn contents have been reported to relieve the grain poisoning effect of Zr on AZ91 alloy. Jafari et al. [71] showed that the grain size of AZ93 alloy was not coarsened when 0.25~0.9% Zr was added, which was ascribed to the higher content of Zn (3%). Compared with lower Zn content (1%), higher Zr content can improve the Zr solubility in Mg alloy, thus improving the grain refinement effect.

### 5. Methods of Improving the Grain Refinement Efficiency of Zr

As is well known, Mg-Zr master alloy with the largest number density of fine Zr particles (1~5 μm) exhibits the best refinement ability [26,31,61]. Therefore, the Zr particle size distribution in the Mg-Zr master alloy needs to be controlled to be as fine and as uniform as possible. To achieve this aim, a new Mg-Zr master alloy with fine Zr particles [14,80] has been developed, and pre-treatments [27,81–87] have been conducted to modify the Mg-Zr master alloys already available. In addition, melt treatment can be conducted to reduce the settling of Zr during the melting of the Mg alloy, thereby improving the Zr grain refinement efficiency [41,49,88–94]. This section briefly summarizes these methods.

#### 5.1. Pretreatments of the Mg-Zr Master Alloy

The severe plastic deformation (SPD) method can generate massive force, breaking the Zr particles into smaller ones, and can be conducted via hot rolling [27,83], equal channel angular extrusion (ECAE) [47,82,83], friction stirring processing (FSP) [84], or crush [85].

Qian [81] first showed that hot rolling effectively fragmented the Zr particle clusters in the Mg-33Zr master alloy into smaller clusters. Sun [27] further verified that eight passes hot rolling effectively crushed the large Zr particles of the Mg-30Zr master alloy into smaller ones. Saha [82] showed that ECAE was able to effectively break up the Zr particles of the Mg-15Zr master alloy. Wang et al. [84] showed that FSP can be used to modify the Zr particle distribution of the Mg-30Zr master alloy. Recently, Wang et al. [85] employed a new method for preparing “powder Mg-Zr master alloy” that consisted of three steps, i.e., mechanically crushing the original Mg-30Zr master alloy block, ball-milling the pieces, and finally sieving to keep particles smaller than 20 μm.

These methods mainly take advantage of mechanical force to refine the Zr particle size. All of these studies proved that the Zr particle size distribution can be modified to become narrow, achieving better distribution. As a result of modification, the settling of Zr particles during melting can be retarded, and a higher soluble Zr content can be obtained. Consequently, the grain refinement efficiency of pretreated Mg-Zr master alloys on pure Mg [81–83], Mg-10Gd-3Y [27], Mg-3Nd-0.2Zn [84] and Mg-14Li-Zn [85] alloys was effectively improved. However, the pretreatment methods have some obvious disadvantages, such as their complicated processes, low productivity, and the SPD molds and tools (FSP probes) being easily broken.

In addition to the SPD methods, a non-equilibrium re-precipitation method via tungsten inert gas arc remelting with ultra-high frequency pulses (UHFP-TIGR) was recently trialed by Xin et al. [86,87]. Figure 12 shows the Zr particle distribution in the UHFP-TIGR-treated Mg-30Zr master alloy. UHFP-TIGR treatment promoted the precipitation of a considerable number of nano-sized Zr particles ( $Zr_{np}$ ) from the supersaturated Mg matrix due to the effect of high temperature, strong stirring, and rapid equilibrium cooling. As a result, the UHFP-TIGR-treated Mg-30Zr master alloy exhibited superior grain refinement efficiency on Mg-9Gd-3Y alloy compared to its untreated counterpart. A similar method was also reported by Zhang et al. [95], who improved the refining efficiency of Al-5Ti-1B master alloy on Al alloys by re-precipitating tiny  $TiB_2$  particles.

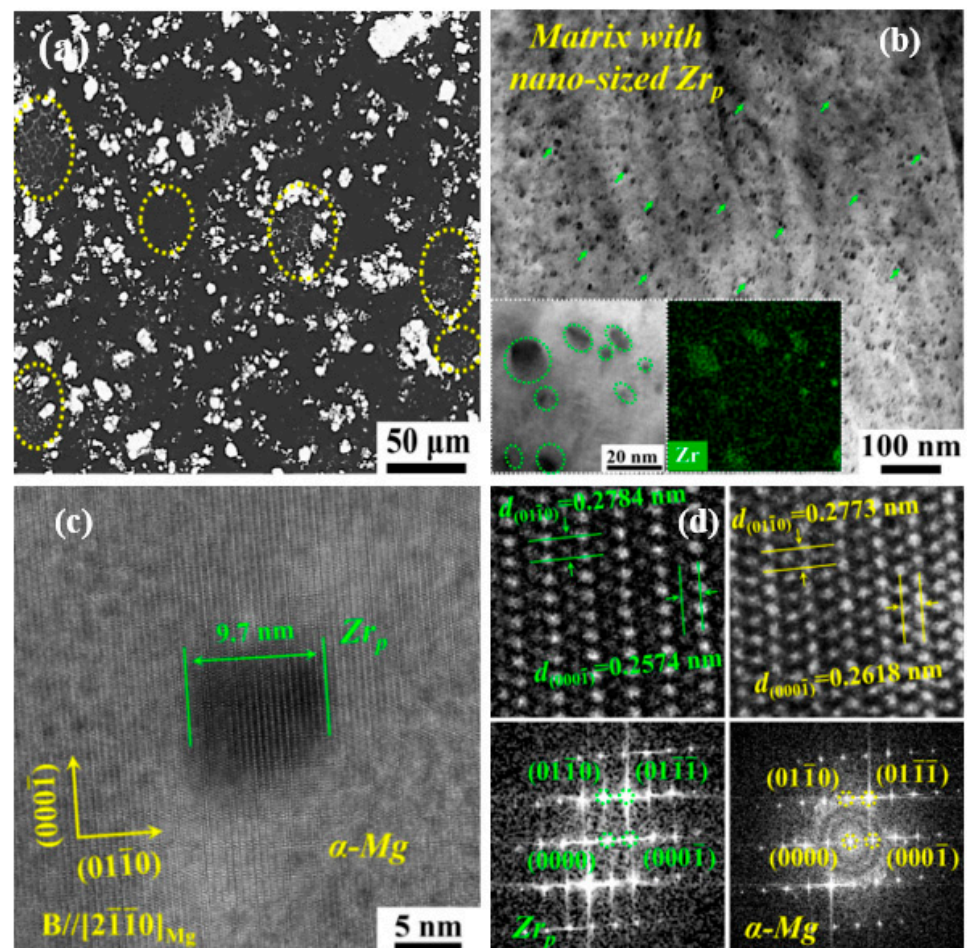


**Figure 12.** Characterization of UHFP-TIGR-treated Mg-30Zr master alloy: (a) SEM BSE image under low magnification; (b) TEM dark-field image; (c,d) HRTEM image with diffraction patterns of nanoscale  $Zr_{np}$  [86]. Reprinted with permission from ref. [86]. Copyright 2022 Elsevier.

## 5.2. Melt Treatments

Melt treatments such as ultrasonic treatment (UST) [88–91], intensive melt shearing (IMS) [41,49,92,93] or low-frequency electro-magnetic stirring (LFEMS) [94] have been tried after the addition of Zr into the Mg alloy melt. Ramirez et al. [88] showed that UTS enhances the effect of grain refinement with Zr (0.5, 1.0 or 1.5Zr) on Mg-3Zn alloy (Figure 13). For instance, the grain size of Mg-3Zn-0.5Zr alloy was about 91.5  $\mu\text{m}$ , which was further refined to 71.9  $\mu\text{m}$  by means of UST. Nagasivamuni et al. [89,90] showed that UST enhances the grain refinement effect of Mg-Zr alloys (0.2, 0.5 or 1.0Zr). The main reason for this is that UST increases the soluble Zr, activates more Zr nucleation particles, and decreases the Zr settling [89,90]. Additionally, another possible reason for this may be that the surfaces of some contaminated Zr particles were cleaned and wetted by UST, facilitating an increase in the number of nucleation sites.

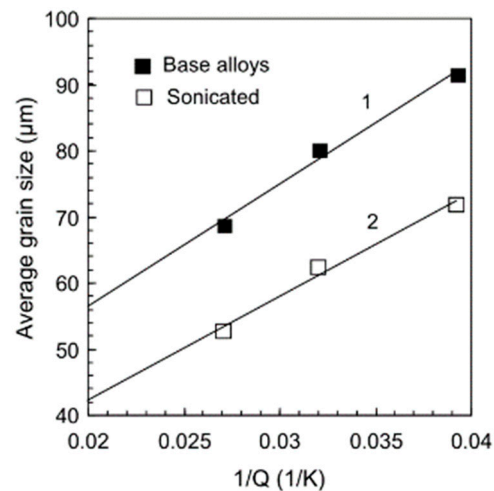


**Figure 13.** Grain size vs.  $1/Q$  for Mg-3Zn-Zr alloys [88]. “Sonicated” = UST; addition of Zr = 0.5, 10.0 and 1.5, respectively. Reprinted with permission from ref. [88]. Copyright 2008 Elsevier.

Das et al. [92] showed that IMS enhances the effect of grain refinement with Zr on Mg-6Zn alloy. The mechanism for this is that IMS deagglomerates and disperses the Zr particle clusters uniformly in the melt, increasing the number density of Zr nucleation particles. However, Peng et al. [39,49,93] showed that IMS makes the effect of grain refinement with Zr more complicated, as a result of the competition between Zr and MgO particles formed in-situ [49]. On the one hand, when Zr content was as low as 0.1%, IMS led to a significant grain refinement of the Mg-0.1Zr alloy. This was because the MgO particles formed in-situ were able to be well dispersed by IMS, resulting in an increase in the number density of MgO nucleating particles. At the same time, the adsorption of the Zr layer on the surface of the MgO particles was enhanced by IMS, leading to an improvement in the nucleating potency of the MgO particles [49]. Thus, the grain refinement effect could be achieved at a relatively lower Zr content (0.1%). On the other hand, when Zr content was just beyond the peritectic point, grain coarsening occurred. This was because the Zr particles underwent a coarsening growth process with the effect of IMS, resulting in the formation of larger Zr particles and a reduction in Zr number density [49]. Thus, grain coarsening was observed. In addition, when Zr content was as high as 2%, the grain was well refined again, because more Zr nucleating particles were supplied.

## 6. Conclusions and Remarks

Zr is the most effective and important grain refiner for Al-free Mg alloys, especially for many high-strength Mg alloys. This review paper summarizes the recent advances in the effect of grain refinement with Zr on Mg alloys in detail, including the alloying process of Zr, the grain refinement mechanism of Zr, the grain refinement behavior of Zr,

and improvements in the grain refinement efficiency of Zr. This review provides a full understanding of the effect of grain refinement with Zr on Mg alloys. The main points of Zr refinement are summarized in Figure 14.

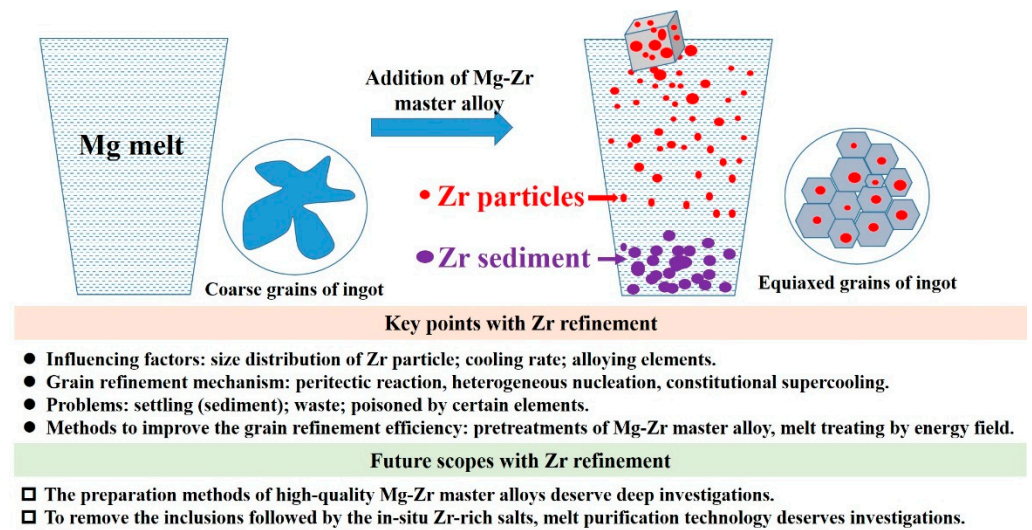


**Figure 14.** The main features of the effect of grain refinement with Zr on Mg alloys.

The main conclusions are as follows:

- (1) Among various methods of introducing Zr into Mg melt, only the Mg-Zr master alloy shows high efficiency. This is because the Mg-Zr master alloy ensures that the interface between the Zr particles and the Mg melt is clean and active, facilitating the diffusion of Zr elements and increased nucleation utilization.
- (2) The grain refinement mechanism is attributed to both heterogeneous nucleation and the constitutional supercooling effect. The perfect crystal match between Zr and Mg, and the high GRF value contribute to the powerful effect of grain refinement with Zr.
- (3) Many factors influence the effect of grain refinement with Zr, including Zr particle settling, the particle size distribution of the Mg-Zr master alloy, cooling rate, and the alloying elements. In particular, the size distribution of the Mg-Zr master alloy has a great influence on the grain refinement efficiency of Zr. The spontaneous settling of Zr particles increases the alloying cost.
- (4) To achieve a better refinement effect and a higher utilization rate of Zr, two methods have been investigated, i.e., pre-treatment of the Mg-Zr master alloy and melt treatment. The newly developed UHFP-TIGR pre-treatment [86] shows remarkable modification effects and remarkable grain refinement efficiency.

However, due to the complicated process of melt treatment or pretreatment of the Mg-Zr master alloy, some work needs to be done in future on tackling the problem of Zr waste at the root and saving expensive Zr resources. The key point is the development of Mg-Zr master alloy with super-fine Zr particles. To achieve this aim, the typical method for preparing the Mg-Zr master alloy, i.e., Mg thermal reduction reaction with Zr-rich halides, should be investigated again in more detail with respect to its thermal dynamic aspects. If the Zr particle size can be controlled to be as small as possible during the reaction, a more economical production of Mg-Zr master alloy will be achieved.

Additionally, if the in-situ method of mixing Zr-rich salts is employed, a suitable purification technology should be developed for removing the salt inclusions in the Mg melt. There are two points worthy of investigation. One is that new fluxes effective in removing inclusions can be developed based on the molten salt system. Another is that complex purification methods such as gas bubbling plus external energy field are deserving of trials.

**Author Contributions:** Conceptualization, M.S. and Y.Z.; methodology, M.S.; investigation, M.S. and D.Y.; resources, L.M., X.L. and S.P.; data curation, M.S. and D.Y.; writing—original draft preparation, M.S.; writing—review and editing, D.Y., L.M. and Y.Z.; supervision, M.S. and Y.Z.; project administration, M.S.; funding acquisition, M.S., Y.Z. and L.M. All authors have read and agreed to the published version of the manuscript.

**Funding:** This research was funded by National Natural Science Foundation of China (NSFC), grant number 51701124, 51901027 and 51901137. The APC was funded by 51701124.

**Data Availability Statement:** Not applicable.

**Conflicts of Interest:** The authors declare no conflict of interest.

## References

1. Karakulak, E. A review: Past, present and future of grain refining of magnesium castings. *J. Magnes. Alloy.* **2019**, *7*, 355–369. [[CrossRef](#)]
2. Song, J.; Chen, J.; Xiong, X.; Peng, X.; Chen, D.; Pan, F. Research advances of magnesium and magnesium alloys worldwide in 2021. *J. Magnes. Alloy.* **2022**, *10*, 863–898. [[CrossRef](#)]
3. Ali, Y.; Qiu, D.; Jiang, B.; Pan, F.; Zhang, M. Current research progress in grain refinement of cast magnesium alloys: A review article. *J. Alloy. Compd.* **2015**, *619*, 639–651. [[CrossRef](#)]
4. StJohn, D.H.; Ma, Q.; Easton, M.A.; Cao, P.; Hildebrand, Z. Grain refinement of magnesium alloys. *Metall. Mater. Trans. A* **2005**, *36*, 1669–1679. [[CrossRef](#)]
5. Sauerwald, F. Das Zustandsdiagramm Magnesium-Zirkonium. *Z. Für Anorg. Chemie.* **1947**, *255*, 212–220. [[CrossRef](#)]
6. Friedrich, H.E.; Mordike, B.L. *Magnesium Technology: Metallurgy, Design Data, Applications*; Springer: Berlin/Heidelberg, Germany, 2006; pp. 128–143.
7. Mo, N.; Tan, Q.; Bermingham, M.; Huang, Y.; Dieringa, H.; Hort, N.; Zhang, M. Current development of creep-resistant magnesium cast alloys: A review. *Mater. Des.* **2018**, *155*, 422–442. [[CrossRef](#)]
8. Sravya, T.; Sankaranarayanan, S.; Abdulhakim, A.; Manoj, G. Mechanical properties of magnesium-rare earth alloy systems: A review. *Metals* **2015**, *5*, 1–39. [[CrossRef](#)]
9. Wu, G.; Wang, C.; Sun, M.; Ding, W. Recent developments and applications on high-performance cast magnesium rare-earth alloys. *J. Magnes. Alloy.* **2021**, *9*, 1–20. [[CrossRef](#)]
10. StJohn, D.H.; Easton, M.A.; Ma, Q.; Taylor, J.A. Grain refinement of magnesium alloys: A review of recent research, theoretical developments, and their application. *Metall. Mater. Trans. A* **2013**, *44*, 2935–2949. [[CrossRef](#)]
11. Easton, M.A.; Ma, Q.; Prasad, A.; StJohn, D.H. Recent advances in grain refinement of light metals and alloys. *Curr. Opin. Solid. State Mater.* **2016**, *20*, 13–24. [[CrossRef](#)]
12. Yu, W.; He, H.; Li, C.; Li, Q.; Liu, Z.; Qin, B. Existing form and effect of zirconium in pure Mg, Mg-Yb, and Mg-Zn-Yb alloys. *Rare Metals* **2009**, *28*, 289–296. [[CrossRef](#)]
13. Emley, E.F. *Principles of Magnesium Technology*; Pergamon Press: Oxford, UK, 1966.
14. Ma, Q.; StJohn, D.H.; Frost, M.T. Magnesium-Zirconium Alloying. U.S. Patent 20050161121A1, 2005.
15. Sun, M.; Wu, G.; Dai, J.; Pang, S.; Ding, W. Current research status of grain refinement effect of Zr on magnesium alloy. *Foundry* **2010**, *59*, 255–259. (In Chinese)
16. Sauerwald, F. Process for the Production of Magnesium-Zirconium Alloys. U.S. Patent 2228781, 14 January 1941.
17. Ball, C.J.P.; Jessup, A.C.; Emley, E.F.; Fisher, P.A. Alloying Composition for Introducing Zirconium into Magnesium. U.S. Patent 2497531, 14 February 1950.
18. Michael, D.W. Magnesium Base Alloys Containing Zirconium. U.S. Patent 2698230, 28 December 1954.
19. Whitehead, D.J.; Frederick, E.E. Alloying of Manganese and Zirconium to Magnesium. U.S. Patent 2919190, 29 December 1959.
20. Sun, M.; Wu, G.; Dai, J.; Wang, W.; Ding, W. Grain refinement behavior of potassium fluozirconate ( $K_2ZrF_6$ ) salts mixture introduced into Mg-10Gd-3Y magnesium alloy. *J. Alloy. Compd.* **2010**, *494*, 426–433. [[CrossRef](#)]
21. Wang, W.; Zhang, M.; Wang, W.; Wang, A.; Li, M. Effect of potassium fluorozirconate salts mixture on the microstructure and mechanical properties of Mg-3Y-3.5Sm-2Zn alloy. *Rare Metal. Mat. Eng.* **2020**, *49*, 1151–1158.
22. Le, Q.; Zhang, Z.; Cui, J. The Preparation Method of Zr-rich Salts Mixture Used for Zr Alloying in Mg Alloy. Chinese Patent 102605200A, 25 July 2012. (In Chinese)
23. Tong, X.; Wu, G.; Zhang, L.; Liu, W.; Ding, W. Achieving low-temperature Zr alloying for microstructural refinement of sand-cast Mg-Gd-Y alloy by employing zirconium tetrachloride. *Mater. Charact.* **2021**, *171*, 110727. [[CrossRef](#)]
24. Viggers, R.F. The Magnesium-Zirconium Alloys. Ph.D. Thesis, Oregon State College, Corvallis, OR, USA, 1950.
25. Sun, M.; Wu, G.; Easton, M.A.; StJohn, D.H.; Abbott, T.; Ding, W. A comparison of the microstructure of three Mg-Zr master alloys and their grain refinement efficiency. In Proceedings of the 9th International Conference on Magnesium Alloys and Their Applications, Vancouver, Canada, 8–12 July 2012; pp. 873–880.
26. Sun, M.; Easton, M.A.; StJohn, D.H.; Wu, G.; Abbott, T.; Ding, W. Grain refinement of magnesium alloys by Mg-Zr master alloys: The role of alloy chemistry and Zr particle number density. *Adv. Eng. Mater.* **2013**, *15*, 373–378. [[CrossRef](#)]

27. Sun, M. Study on Grain Refinement Behavior of Mg-Gd-Y Magnesium Alloy by Zirconium. Ph.D. Thesis, Shanghai Jiao Tong University, Shanghai, China, 2012. (In Chinese)
28. Liu, H.; Ning, Z.; Cao, F.; Zhang, Y.; Sun, J. Effect of melting process on Zr content and grain refinement in ZE41A alloy. *Adv. Mat. Res.* **2011**, *284–286*, 1651–1655. [[CrossRef](#)]
29. Ma, Q.; Graham, D.; Zheng, L.; StJohn, D.H.; Frost, M.T. Alloying of pure magnesium with Mg-33.3 wt.% Zr master alloy. *Mater. Sci. Technol.* **2003**, *19*, 156–162. [[CrossRef](#)]
30. Ma, Q.; Zheng, L.; Graham, D.; Frost, M.T.; StJohn, D.H. Settling of undissolved zirconium particles in pure magnesium melts. *J. Light Met.* **2001**, *1*, 157–165.
31. Ma, Q.; Das, A. Grain refinement of magnesium alloys by zirconium: Formation of equiaxed grains. *Scr. Mater.* **2006**, *54*, 881–886. [[CrossRef](#)]
32. Tamura, Y.; Kono, N.; Motegi, T.; Sato, E. Grain refining of pure magnesium by adding Mg-Zr master alloy. *J. Jpn. Inst. Met.* **1997**, *47*, 679–684. (In Japanese)
33. Qiu, D.; Zhang, M.; Taylor, J.A.; Kelly, P.M. A new approach to designing a grain refiner for Mg casting alloys and its use in Mg-Y-based alloys. *Acta Mater.* **2009**, *57*, 3052–3059. [[CrossRef](#)]
34. Dai, J.; Easton, M.A.; Zhang, M.; Qiu, D.; Xiong, X.; Liu, W.; Wu, G. Effects of cooling rate and solute content on the grain refinement of Mg-Gd-Y alloys by aluminum. *Metall. Mater. Trans. A* **2014**, *45*, 4665–4678. [[CrossRef](#)]
35. Wang, C.; Dai, J.; Liu, W.; Zhang, L.; Wu, G. Effect of Al additions on grain refinement and mechanical properties of Mg-Sm alloys. *J. Alloy. Compd.* **2015**, *620*, 172–179. [[CrossRef](#)]
36. Ma, Q.; StJohn, D.H.; Frost, M.T. Effect of soluble and insoluble zirconium on the grain refinement of magnesium alloys. *Mater. Sci. Forum* **2003**, *419–422*, 593–598. [[CrossRef](#)]
37. Ma, Q.; StJohn, D.H.; Frost, M.T. Characteristic zirconium-rich coring structures in Mg-Zr alloys. *Scr. Mater.* **2002**, *46*, 649–654. [[CrossRef](#)]
38. Ma, Q.; StJohn, D.H. Grain nucleation and formation in Mg-Zr alloys. *Int. J. Cast. Metal. Res.* **2009**, *22*, 256–259. [[CrossRef](#)]
39. Ma, Q.; StJohn, D.H.; Frost, M.T. Zirconium alloying and grain refinement of magnesium alloys. In Proceedings of the Magnesium Technology 2003, San Diego, CA, USA, 2–6 March 2003; pp. 209–214, Edited by Howard I. Kaplan.
40. Ramachandran, T.R.; Sharma, P.K.; Balasubramanian, K. Grain refinement of light alloys. In Proceedings of the 68th WFC-World Foundry Congress, Chennai, India, 7–10 February 2008; pp. 189–193.
41. Peng, G.; Wang, Y.; Chen, K.; Chen, S. Improved Zr grain refining efficiency for commercial purity Mg via intensive melt shearing. *Int. J. Cast. Metal. Res.* **2017**, *30*, 374–378. [[CrossRef](#)]
42. Ma, Q. Heterogeneous nucleation on potent spherical substrates during solidification. *Acta Mater.* **2007**, *55*, 943–953. [[CrossRef](#)]
43. StJohn, D.H.; Ma, Q.; Easton, M.A.; Cao, P. The Interdependence Theory: The relationship between grain formation and nucleant selection. *Acta Mater.* **2011**, *59*, 4907–4921. [[CrossRef](#)]
44. Li, J.; Chen, R.; Ma, Y.; Ke, W. Effect of Zr modification on solidification behavior and mechanical properties of Mg-Y-RE (WE54) alloy. *J. Magnes. Alloy.* **2013**, *1*, 346–351. [[CrossRef](#)]
45. Zhao, Y.; Pu, Z.; Wang, L.; Liu, D. Modeling of grain refinement and nucleation behavior of Mg-4Y-0.5Zr (wt.%) alloy via cellular automaton model. *Int. J. Metalcast.* **2022**, *16*, 945–961. [[CrossRef](#)]
46. Tamura, Y.; Kono, N.; Motegi, T.; Sato, E. Grain refining mechanism and casting structure of Mg-Zr alloy. *J. Jpn. Inst. Met.* **1998**, *48*, 185–189. (In Japanese)
47. Saha, P. An Analysis of the Grain Refinement of Magnesium by Zirconium. Ph.D. Thesis, The University of Alabama, Tuscaloosa, AL, USA, 2010. ProQuest Dissertations Publishing.
48. Saha, P.; Viswanathan, S. Grain refinement of magnesium by zirconium: Characterization and analysis. In Proceedings of the American Foundry Society (AFS) Proceedings 2011, Dayton, IL, USA, 10–12 October 2011; pp. 175–180.
49. Peng, G.S.; Wang, Y.; Fan, Z. Competitive heterogeneous nucleation between Zr and MgO particles in commercial purity magnesium. *Metall. Mater. Trans. A* **2018**, *49*, 2182–2192. [[CrossRef](#)]
50. Yang, W.; Ji, S.; Zhang, R.; Zhang, J.; Liu, L. Abnormal grain refinement behavior in high-pressure die casting of pure Mg with addition of Zr as grain refiner. *JOM* **2018**, *70*, 2555–2560. [[CrossRef](#)]
51. Yang, W.; Liu, L.; Zhang, J.; Ji, S.; Fan, Z. Heterogeneous nucleation in Mg-Zr alloy under die casting condition. *Mater. Lett.* **2015**, *160*, 263–267. [[CrossRef](#)]
52. Abdallah, E.; Francesco, D.; Comondore, R.; Dimitry, S. Observing the effect of grain refinement on crystal growth of Al and Mg alloys during solidification using in-situ neutron diffraction. *Metals* **2022**, *12*, 793. [[CrossRef](#)]
53. Han, Q. The role of solutes in grain refinement of hypoeutectic magnesium and aluminum alloys. *J. Magnes. Alloy* **2022**, *in press*. [[CrossRef](#)]
54. StJohn, D.H.; Cao, P.; Ma, Q.; Easton, M.A. A new analytical approach to reveal the mechanisms of grain refinement. *Adv. Eng. Mater.* **2007**, *9*, 739–749. [[CrossRef](#)]
55. Easton, M.A.; StJohn, D.H. A model of grain refinement incorporating alloy constitution and potency of heterogeneous nucleant particles. *Acta Mater.* **2001**, *49*, 1867–1878. [[CrossRef](#)]
56. Fan, Z.; Gao, F.; Wang, Y.; Men, H.; Zhou, L. Effect of solutes on grain refinement. *Prog. Mater. Sci.* **2022**, *123*, 100809. [[CrossRef](#)]
57. Peng, Z.K.; Zhang, X.M.; Chen, J.-M.; Xiao, Y.; Jiang, H. Grain refining mechanism in Mg-9Gd-4Y alloys by zirconium. *Mater. Sci. Technol.* **2005**, *21*, 722–726. [[CrossRef](#)]

58. Zhang, D.; Qiu, D.; Zhu, S.; Dargusch, M.; StJohn, D.H.; Easton, M.A. Grain refinement in laser remelted Mg-3Nd-1Gd-0.5Zr alloy. *Scr. Mater.* **2020**, *183*, 12–16. [[CrossRef](#)]
59. Ma, Q. Creation of semisolid slurries containing fine and spherical particles by grain refinement based on the Mullins-Sekerka stability criterion. *Acta Mater.* **2006**, *54*, 2241–2252. [[CrossRef](#)]
60. Chen, Y.; Zhang, L.; Liu, W.; Wu, G.; Ding, W. Preparation of Mg-Nd-Zn-(Zr) alloys semisolid slurry by electromagnetic stirring. *Mater. Des.* **2016**, *95*, 398–409. [[CrossRef](#)]
61. Ma, Q.; StJohn, D.H.; Frost, M.T. Heterogeneous nuclei size in magnesium- zirconium alloys. *Scr. Mater.* **2004**, *50*, 1115–1119. [[CrossRef](#)]
62. Liu, H.; Ning, Z.; Cao, F.; Meng, Z.; Sun, J. Effect of cooling condition on Zr-rich core formation and grain size in Mg alloy. *Adv. Mat. Res.* **2011**, *189–193*, 3920–3924. [[CrossRef](#)]
63. Sun, M.; Stjohn, D.H.; Easton, M.A.; Wang, K.; Ni, J. Effect of cooling rate on the grain refinement of Mg-Y-Zr alloys. *Metall. Mater. Trans. A* **2020**, *51*, 482–496. [[CrossRef](#)]
64. Kabirian, F.; Mahmudi, R. Effects of zirconium additions on the microstructure of as-cast and aged AZ91 magnesium alloy. *Adv. Eng. Mater.* **2009**, *11*, 189–193. [[CrossRef](#)]
65. Balasubramani, N.; Wang, G.; StJohn, D.H.; Dargusch, M.S. The poisoning effect of Al and Be on Mg-1 wt.% Zr alloy and the role of ultrasonic treatment on grain refinement. *Front. Mater.* **2019**, *10*, 322. [[CrossRef](#)]
66. Cao, P.; Ma, Q.; StJohn, D.H.; Frost, M.T. Uptake of iron and its effect on grain refinement of pure magnesium by zirconium. *Mater. Sci. Technol.* **2004**, *20*, 585–592. [[CrossRef](#)]
67. Cao, P.; Qian, M.; StJohn, D.H. Grain coarsening of magnesium alloys by beryllium. *Scr. Mater.* **2004**, *51*, 647–651. [[CrossRef](#)]
68. Chang, S.Y.; Tezuka, H.; Kamio, A. Mechanical properties and structure of ignition-proof Mg-Ca-Zr alloys produced by squeeze casting. *Mater. Trans. JIM* **1997**, *38*, 526–535. [[CrossRef](#)]
69. Hildebrand, Z.; Qian, M.; StJohn, D.H.; Frost, M.T. Influence of zinc on the soluble zirconium content in magnesium and the subsequent grain refinement by zirconium. In Proceedings of the Magnesium Technology 2004, Warrendale, PA, USA, 14–18 March 2004; pp. 241–245.
70. Li, P.; Hou, D.; Han, E.; Chen, R.; Shan, Z. Solidification of Mg-Zn-Zr alloys: Grain growth restriction, dendrite coherency and grain size. *Acta Metall. Sin.* **2020**, *33*, 1477–1486. [[CrossRef](#)]
71. Jafari, H.; Amiryavari, P. The effects of zirconium and beryllium on microstructure evolution; mechanical properties and corrosion behaviour of as-cast AZ63 alloy. *Mat. Sci. Eng. A* **2016**, *654*, 161–168. [[CrossRef](#)]
72. Tamura, Y.; Motegi, T.; Kono, N.; Sato, E. Effect of minor elements on grain size of Mg-9%Al alloy. *Mater. Sci. Forum* **2000**, *350–351*, 199–204. [[CrossRef](#)]
73. Cao, P.; Ma, Q.; StJohn, D.H. Native grain refinement of magnesium alloys. *Scr. Mater.* **2005**, *53*, 841–844. [[CrossRef](#)]
74. Miyahara, Y.; Matsubara, K.; Horita, Z.; Langdon, T.G. Grain refinement and superplasticity in a magnesium alloy processed by equal-channel angular pressing. *Metall. Mater. Trans. A* **2005**, *36*, 1705–1711. [[CrossRef](#)]
75. Kabirian, F.; Mahmudi, R. Effects of Zr additions on the microstructure and impression creep behavior of AZ91 magnesium alloy. *Metall. Mater. Trans. A* **2010**, *41*, 3488–3498. [[CrossRef](#)]
76. Ma, Q.; Hildebrand, Z.C.G.; StJohn, D.H. The loss of dissolved zirconium in zirconium-refined magnesium alloys after remelting. *Metall. Mater. Trans. A* **2009**, *40*, 2470–2479. [[CrossRef](#)]
77. Davis, B.; O'Reilly, K. Electron probe micro analysis of sedimented zirconium particles in magnesium. In *Proceedings of the 6th International Conference Magnesium Alloys and Their Applications*; Wiley: New York, NY, USA, 2003; pp. 242–247. [[CrossRef](#)]
78. Prasad, A.; Uggowitzer, P.J.; Shi, Z.; Atrens, A. Production of high purity Mg-X rare earth binary alloys using Zr. *Mater. Sci. Forum* **2013**, *765*, 301–305. [[CrossRef](#)]
79. Xing, F.; Guo, F.; Su, J.; Zhao, X.; Cai, H. The existing forms of Zr in Mg-Zn-Zr magnesium alloys and its grain refinement mechanism. *Mater. Res. Express* **2021**, *8*, 066516. [[CrossRef](#)]
80. Ma, Q.; StJohn, D.H.; Frost, M.T. A new zirconium-rich master alloy for the grain refinement of magnesium alloys. In *Magnesium: Proceedings of the 6th International Conference Magnesium Alloys and Their Applications*; Wiley: New York, NY, USA, 2003; pp. 706–712. [[CrossRef](#)]
81. Ma, Q.; StJohn, D.H.; Frost, M.T.; Barnett, M.R. Grain refinement of pure magnesium using rolled Zirmax® master alloy (Mg-33.3Zr). In Proceedings of the Magnesium: Proceedings of Magnesium Technology 2003, San Diego, CA, USA, 2–6 March 2003; pp. 215–220.
82. Viswanathan, S.; Saha, P.; Foley, D.; Hartwig, K.T. Engineering a more efficient zirconium grain refiner for magnesium. In *Magnesium Technology 2011*; Springer: Berlin/Heidelberg, Germany; pp. 559–564.
83. Viswanathan, S.; Saha, P.; Foley, D.; Hartwig, K.T. Developing an improved zirconium grain refiner for magnesium. In Proceedings of the American Foundry Society (AFS) Proceedings 2011, Dayton, IL, USA, 10–12 October 2011; p. 11-067.
84. Wang, C.; Sun, M.; Zheng, F.; Peng, L.; Ding, W. Improvement in grain refinement efficiency of Mg-Zr master alloy for magnesium alloy by friction stir processing. *J. Magnes. Alloy.* **2014**, *2*, 239–244. [[CrossRef](#)]
85. Wang, L.; Guan, H.; Wu, G.; Pan, Y.; Sun, S. A new approach to improving the macrosegregation in zirconium-containing magnesium-lithium alloy. *Materialwiss. Werkstofftechnol.* **2018**, *49*, 1125–1134. [[CrossRef](#)]
86. Tong, X.; Wu, G.; Easton, M.A.; Sun, M.; StJohn, D.H.; Jiang, R.; Qi, F. Exceptional grain refinement of Mg-Zr master alloy treated by tungsten inert gas arc re-melting with ultra-high frequency pulses. *Scr. Mater.* **2022**, *215*, 114700. [[CrossRef](#)]

87. Tong, X.; Wu, G.; Zhang, L. A Pretreatment Method to Improve the Refining Effect of Mg-Zr Master Alloy on Mg alloy. Chinese Patent 111872517B, 20 July 2021. (In Chinese)
88. Ramirez, A.; Ma, Q.; Davis, B.; Wilks, T.; StJohn, D.H. Potency of high-intensity ultrasonic treatment for grain refinement of magnesium alloys. *Scr. Mater.* **2008**, *59*, 19–22. [[CrossRef](#)]
89. Nagasivamuni, B.; Wang, G.; StJohn, D.H.; Dargusch, M.S. Effect of ultrasonic treatment on the alloying and grain refinement efficiency of a Mg-Zr master alloy added to magnesium at hypo- and hyper-peritectic compositions. *J. Cryst. Growth* **2019**, *512*, 20–32. [[CrossRef](#)]
90. Nagasivamuni, B.; Wang, G.; Easton, M.A.; StJohn, D.H.; Dargusch, M.S. A comparative study of the role of solute, potent particles and ultrasonic treatment during solidification of pure Mg, Mg-Zn and Mg-Zr alloys. *J. Magnes. Alloy.* **2021**, *9*, 829–839. [[CrossRef](#)]
91. Xiao, L.; Tian, Y.; Li, Z.; Zou, W.; Yuan, Y.; Li, B.; Wang, X.; Zhang, X. A Method of Preparing Magnesium Zirconium Master Alloy by Ultrasonic Treatment. CN105385863A, 31 May 2017. (In Chinese)
92. Das, A.; Liu, G.; Fan, Z. Investigation on the microstructural refinement of an Mg-6 wt.% Zn alloy. *Mater. Sci. Eng. A* **2006**, *419*, 349–356. [[CrossRef](#)]
93. Peng, G.; Wang, Y.; Fan, Z. Effect of intensive melt shearing and Zr content on grain refinement of Mg-0.5Ca-xZr alloys. *Mater. Sci. Forum* **2013**, *765*, 336–340. [[CrossRef](#)]
94. Wang, C.; Dong, Z.; Li, K.; Sun, M.; Wu, J.; Wang, K.; Wu, G.; Ding, W. A novel process for grain refinement of Mg-RE alloys by low frequency electro-magnetic stirring assisted near-liquidus squeeze casting. *J. Mater. Process. Technol.* **2022**, *303*, 117537. [[CrossRef](#)]
95. Zhang, L.; Jiang, H.; He, J.; Zhao, J. Improved grain refinement in aluminium alloys by re-precipitated TiB<sub>2</sub> particles. *Mater. Lett.* **2022**, *312*, 131657. [[CrossRef](#)]